GC/MS and LC/MS-based Tissue Metabolomic Analysis Detected Increased Levels of Antioxidant Metabolites in Colorectal Cancer

MEGUMI KIBI[1], SHIN NISHIUMI[1], TAKASHI KOBAYASHI[1],
YUZO KODAMA[1] and MASARU YOSHIDA[1,2,3,*]

[1] Division of Gastroenterology, Department of Internal Medicine, Kobe University Graduate School of Medicine, Kobe, Japan;
[2] Division of Metabolomics Research, Department of Internal Related, Kobe University Graduate School of Medicine, Kobe, Japan;
[3] AMED-CREST, AMED, Kobe, Japan.   *Corresponding author

Late-stage colorectal cancer is resistant to current treatments. Understanding the biological processes responsible for the development and progression of colorectal cancer could aid the development of new diagnostic and treatment approaches. We used gas chromatography/mass spectrometry and liquid chromatography/mass spectrometry-based metabolomic analysis to measure metabolite levels in pairs of colorectal cancer tissue samples and samples of the adjacent macroscopically normal mucosal tissue from 10 colon cancer patients. Regarding nucleotide metabolomic intermediates, the colorectal cancer tissue contained lower levels of ribulose 5-phosphate and higher levels of xanthine, adenine, and hypoxanthine than the normal tissue. The levels of antioxidant metabolites, such as sulfur-containing amino acids, were also significantly higher in the colorectal cancer tissue. The level of tryptophan was decreased, and the levels of molecules downstream of the tryptophan pathway, such as kynurenine and quinolinic acid, which protect colorectal cancer against the host's immune system and function in *de novo* nicotinamide adenine dinucleotide synthesis, were increased in the colorectal cancer tissue. The colorectal cancer tissue samples also contained higher levels of lysophospholipids and fatty acids, especially stearic acid and polyunsaturated fatty acids, including arachidonic acid and docosahexaenoic acid. Thus, understanding these cancer-specific alterations could make it possible to detect colorectal cancer early and aid the development of additional treatments for the disease, leading to improvements in colorectal cancer patients' quality of life.

INTRODUCTION

Among various forms of cancer, colorectal cancer (CRC) ranks third in terms of incidence and second in terms of mortality. In addition, it was estimated that over 1.8 million new CRC cases and 881,000 deaths would occur in 2018 [1]. Despite surgical advances and the widespread adoption of combined-modality treatment, the 5-year survival rate of CRC rarely exceeds 60%. Our understandings of the biological processes involved in the development and progression of CRC would aid the development of new diagnostic and prognostic approaches for the disease. The human genome had been completely determined by the end of 2003. Then, "clinical proteomics" was developed, and next many researchers tried to utilize proteomic analysis to the medical field in order to find effective diagnostic markers and provide further information about pathological conditions. Furthermore, metabolomics, which is the comprehensive study of low-molecular-weight metabolites, has also been developed. The metabolome, which is the endpoint of the omics cascade, is closest to actual cancer phenotypes. Profiling the metabolome of CRC and the adjacent macroscopically normal mucosal tissue can provide direct and accurate molecular information about metabolism. In addition, it allows tumors to be characterized and metabolite-based prognostic models to be built, and increases understanding regarding the potential reciprocal relationships between metabolic networks and the underlying mechanisms of CRC development and progression. For example, in our previous study, serum metabolome analysis was used to identify metabolite biomarker candidates that could be used to diagnose CRC [2]. Multiple logistic regression analysis of various metabolite biomarkers from the results of plasma metabolome analysis of early stage CRC patients was carried out, and a stage 0/I/II colorectal cancer prediction model was established [3]. Michael *et al* [4] revealed that elevated levels of carnitine, certain fatty acids (FA), and membrane components at all stages of the CRC tissue include precancerous polyps and several FA, acylcarnitines (AC), and some membrane components were unexpectedly found to be decreased in the later stage CRC compared with the earlier stage CRC, suggesting that metabolite signatures have the potential to be used as new biomarkers for disease

Phone: +81-78-382-6305   Fax: +81-78-382-6309   E-mail: myoshida@med.kobe-u.ac.jp

progression. Hirayama *et al.* performed quantitative metabolite profiling of CRC tissue and stomach cancer tissue, and showed significant organ specific differences in the levels of TCA cycle intermediates, which reflected CRC tissue on aerobic respiration according to oxygen availability. Therefore, cancer cells preferentially use glucose because of their intrinsic metabolic characteristics and microenvironmental aspects such as hypoxia and poor blood supply and high glucose consumption by CRC cells [5]. Thus, we hypothesized that CRC tissue has cancer specific systems to protect themselves from hypoxia and poor blood supply. To investigate the cancer specific protection systems, the CRC tissue metabolome analysis will improve the better understanding of the altered CRC metabolism and can help discover novel agents to treat or even prevent CRC.

In the current study, we obtained pairs of tissue samples of CRC and normal mucosal tissue (each pair was taken from the same resected specimen) from 10 CRC patients and then subjected them to metabolomic analysis. We performed metabolomic analysis using gas chromatography/mass spectrometry (GC/MS) (to analyze water-soluble metabolites); liquid chromatography/mass spectrometry (LC/MS), which was performed with a pentafluorophenylpropyl column (to analyze cations); an octadecylsilylated (C18) silica column with an ion-pair reagent (to analyze anions); and an octadecylsilylated (C18) silica column (to analyze lipids) to measure the metabolite levels in the CRC tissue samples and matched normal tissue samples. Compared with the normal tissue samples, the CRC tissue samples exhibited higher levels of various metabolites, including glycolytic intermediates; amino acids, such as sulfur-containing amino acids (SAA); organic acids related to the kynurenine pathway; nucleotides, including xanthine; and some vitamins, such as pantothenic acid and ascorbic acid. The levels of several key metabolites involved in energy metabolism, such as glucose and nucleoside triphosphates, were lower in the CRC tissue samples. On the other hand, the levels of most lysophospholipids and FA, especially unsaturated FA, were higher in the CRC tissue samples.

MATERIALS AND METHODS

Samples

This study was approved by the ethics committee of Kobe University Graduate School of Medicine (permission#: 782). The human samples were used in accordance with the guidelines of each hospital, and written informed consent was obtained from all subjects. From 2009 to 2011, biopsy samples were collected from 10 patients with CRC at Kobe University Hospital during operations performed at the surgery department and kept on ice. The patients were diagnosed via microscopy, biopsy, or surgical resection and classified using the sixth edition of the International Union Against Cancer classification. All eligible CRC patients had their diagnoses and staging verified according to the TNM Classification of Malignant Tumors. No complications arose in any case. The subjects' information is summarized in the Results section. The surgically excised tissue samples were immediately transferred to ice and then stored at -80°C to quench any enzymatic metabolism, to minimize postmortem degradation, and to avoid sample contamination by the surrounding blood cells.

GC/MS procedures

The CRC and normal tissue samples collected from the patients were stored at -80°C until they were used. To extract low-molecular-weight metabolites, 10 mg of each sample was transferred to a clean tube and homogenized in 1,000 µL of a solvent mixture (MeOH:H_2O:$CHCl_3$=2.5:1:1). The extraction of low-molecular-weight metabolites and GC/MS measurements were carried out according to the methods described in our previous report [6]. The GC/MS analysis was conducted using a GCMS-QP2010 Ultra (Shimazu Co., Kyoto, Japan). The data processing was performed using the software MetAlign (Wageningen UR, https://www.wur.nl/nl/Onderzoek-Resultaten/Onderzoeksinstituten/RIKILT/show-rikilt/MetAlign.htm) and in-house analytical software (AIoutput), as described in our previous reports [2][6][7]. In the semiquantitative analysis, the peak height of each ion was calculated and normalized to the peak height of 2-isopropylmalic acid as an internal standard. Names were assigned to each metabolite peak based on the method described in our previous report [6].

LC/MS procedures

For the LC/MS-based hydrophilic metabolite analysis, 10 mg of tissue was mixed with 900 µl of a solvent mixture (MeOH:H_2O:$CHCl_3$=2.5:1:1) containing 1 µM 2-bromohypoxanthine and 1 µM 10-camphorsulfonic acid as internal standards, and then the solution was shaken at 1,400 rpm for 30 min at 37°C, before being centrifuged at 16,000 g for 3 min at 4°C. Six hundred and thirty µl of the resultant supernatant was transferred to a clean tube, and 280 µl of distilled water was added to the tube. After being mixed, the solution was centrifuged at 16,000 g for 5 min at 4°C, and 500 µl of the resultant supernatant was passed through an ultrafiltration filter, before being subjected to centrifugation at 14,000 g for 60 min at 4°C. The collected solution was dried by centrifugal concentration and lyophilization, and then reconstituted with 100 µl of water. The resultant supernatant was subjected to LC/MS analysis. For the LC/MS-based lipid analysis, 5 mg of tissue was mixed with 80 µl of MeOH and 10 µl of 500 ppb dilauroylphosphatidylcholine (12:0/12:0; Avanti Polar Lipids, AL,

USA) as an internal standard dissolved in MeOH, and then the solution was centrifuged at 16,000 g for 5 min at 4°C. The resultant supernatant was subjected to LC/MS analysis.

According to the method described in a previous report [7], the LC/MS analysis was carried out using a Nexera LC system (Shimadzu Co.). The cation metabolites were separated using a pentafluorophenyl column (Discovery HS F5; Sigma, Tokyo, Japan) with a guard column, while the anion metabolites were separated using an octadecylsilylated silica column (InertSustain C18; GL Sciences, Tokyo, Japan). To identify the hydrophilic metabolites (cation and anion metabolites), the m/z value and retention time of each peak were compared with those of authentic chemical standards that had been analyzed using the same analytical methods. The peak area of each metabolite was normalized to the peak area of the internal standard. Lipids were separated using an octadecylsilylated silica column (InertSustain C18) with a guard column. The lipid analysis for phosphatidylcholines (PC), phosphatidylethanolamines (PE), lysophosphatidylcholines (LPC), lysophosphatidylethanolamines (LPE), and AC was mainly performed based upon the metabolites' physicochemical properties and/or their spectral similarity with the data in public/commercial spectral libraries, because no chemical reference standards for lipids were almost available. The lipid analysis for FA, cholesterol (CHO), and bile acids was performed based upon available chemical reference standards (Avanti Polar Lipids Inc, Alabaster, AL; Sigma-Aldrich, St. Louis).

Statistical analysis

The metabolite data obtained from GC/MS and LC/MS were divided by tissue weight and adjusted using the internal standard data. In the GC/MS- and LC/MS-based analyses, the levels of tissue metabolites were compared between the CRC and normal tissue samples using the Mann-Whitney U test (*$p < 0.05$; **$p < 0.01$; ***$p < 0.005$).

RESULTS

Tissue samples from 10 patients, including 8 males and 2 females, were analyzed. The patients' mean age was 59.1 years old. One patient had CRC of both the sigmoid colon and rectum, 1 patient had CRC of both the ascending colon and rectum, and 5 and 3 patients had CRC of the sigmoid colon and rectum respectively. There were 1, 4, 0, and 5 patients with stage I, II, III, and IV disease, respectively.

We performed GC/MS or LC/MS-based cation, anion, and lipid analyses. Our GC/MS-based metabolomic analysis system, which mainly targeted water-soluble metabolites, detected 114 metabolites, and the levels of 14 metabolites differed significantly between the CRC and normal tissue samples. Among these 14 metabolites, the levels of 13 and 1 metabolites were significantly higher and lower in the CRC tissue samples, respectively. In the LC/MS-based lipid analysis, we detected 31 FA, 7 AC, 73 PC, 56 PE, 42 LPC, 21 LPE, and 1 CHO. We also could not detect bile acids. The levels of 26 of the 31 FA were significantly increased in the CRC tissue samples. The levels of 5 AC were significantly increased in the CRC tissue samples. The levels of 27 and 3 PC were significantly increased and decreased in the CRC tissue samples, respectively. The levels of 15 and 6 PE were significantly increased and decreased in the CRC tissue samples, respectively. The levels of 35 LPC were significantly increased in the CRC tissue samples. The levels of 18 LPE were significantly increased in the CRC tissue samples. Interestingly, none of the LPC or LPE displayed significantly decreased levels in the CRC tissue samples (**Table I, Figure 1**). Most of the FA that exhibited increased levels in the CRC tissue samples were unsaturated FA. The polyunsaturated PC tended to exhibit increased levels in the CRC tissue samples. The levels of polyunsaturated PE differed significantly in the CRC tissue samples (**Figure 1**). The levels of Arachidonic acid (AA) and Eicosapentaenonic acid (EPA) were increased in the CRC tissue samples (**Table I**). EPA is one of important polyunsaturated FA which antagonistically works to AA, so we calculated the ratio of EPA to AA. As a result, the average EPA/AA ratio was significantly lower in the CRC tissue samples (EPA/AA ratio=0.13) compared with the normal tissues (EPA/AA ratio=0.15).
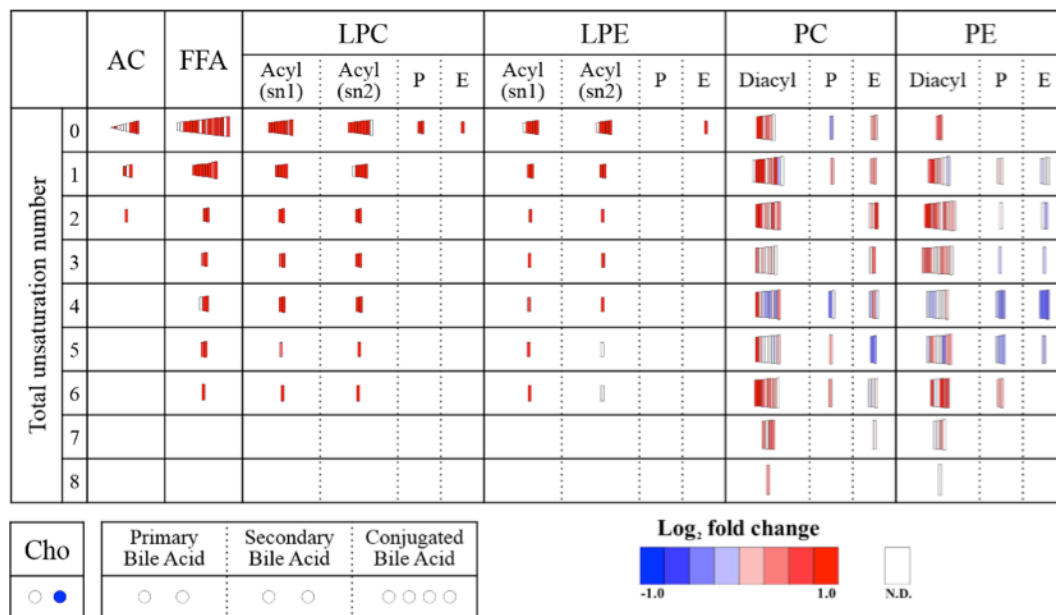
During the cation and anion analyses, 59 cation metabolites and 55 anion metabolites were detected. In the cation analysis, the levels of 7 and 1 metabolites were significantly higher and lower in the CRC tissue samples, respectively. In the anion analysis, the levels of 4 and 3 metabolites were higher and lower in the CRC tissue samples, respectively.

The changes in the levels of the metabolites involved in glycolysis, the pentose phosphate pathway, the tricarboxylic acid (TCA) cycle, glutathione biosynthesis, and amino acid pathways are shown on a metabolic pathway map in **Figure 2A**. The changes in the levels of the metabolites involved in nucleotide metabolism pathways are shown in **Figure 2B**. After mapping the metabolites into general biochemical pathway illustrated in the Kyoto Encyclopedia of Genes and Genomes [8], it became clear that the levels of intermediates involved in glycolysis, the pentose pathway, glutathione biosynthesis, and the tryptophan kynurenine (TK) pathway were significantly higher in the CRC tissue samples. The levels of metabolites involved in the propanediol pathway via dihydroxyacetone phosphate were not changed (**Figure 2A**). As for the levels of metabolites involved in

Table I. List of lipids with the significant differences between colorectal cancer and normal tissues determined by LC/MS-based lipid analysis.
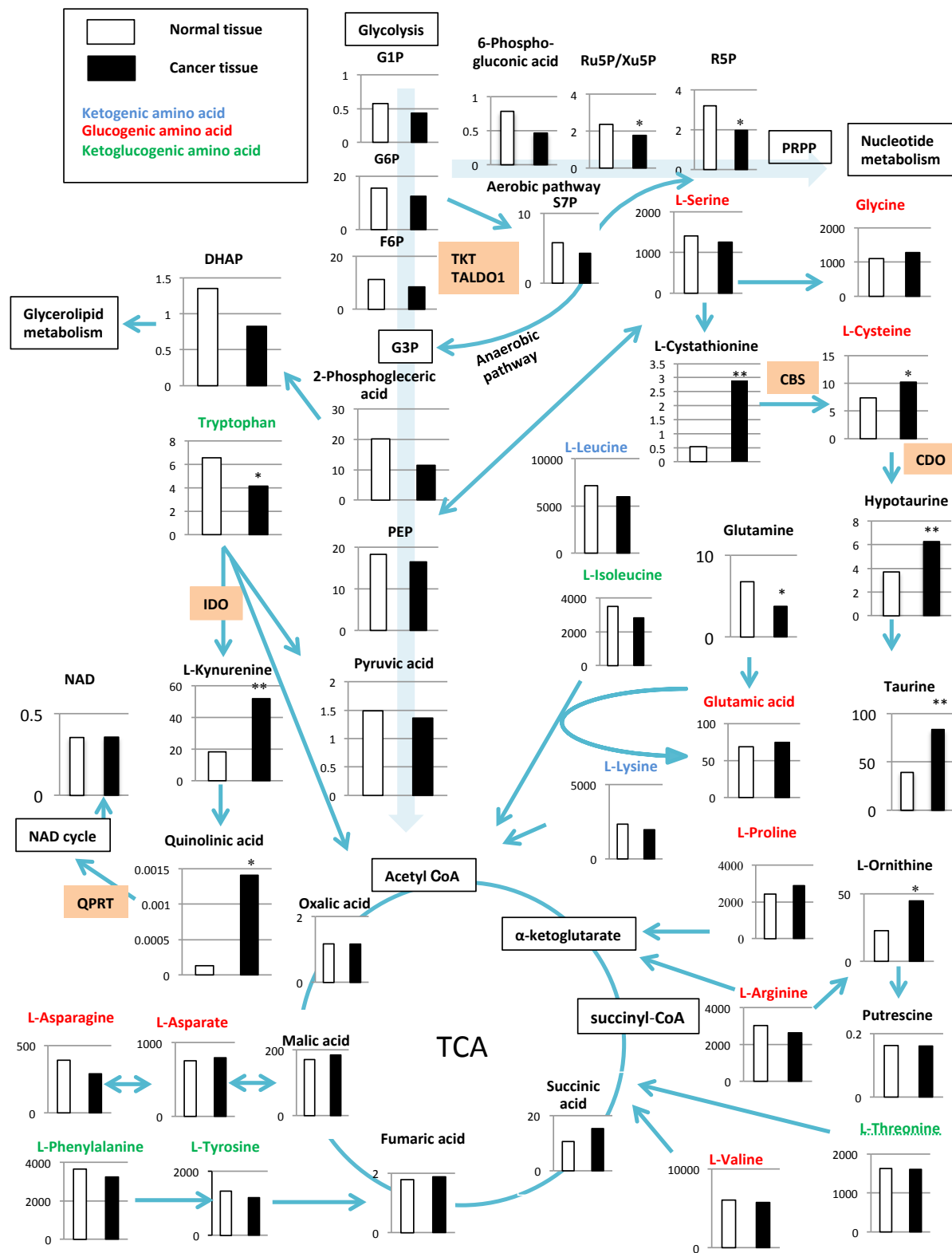
FA	c/n	P value
FA 14:0	2.01	0.0039
FA 14:1 (n-5)	2.05	0.002
FA 15:0	2.08	0.0488
FA 16:0	2.04	0.0039
FA 16:1 (n-7)	2.79	0.0059
FA 17:0	2.26	0.0137
FA 17:1 (n-7)	3	0.0059
FA 18:0	2.08	0.002
FA 18:1 (n-9)	2.32	0.0059
FA 18:1 (n-9)&(n-7)	2.33	0.0059
FA 18:2 (n-6)	2.27	0.0098
FA 18:3 (n-3)&(n-6)	1.7	0.0488
FA 20:0	1.97	0.002
FA 20:1 (n-9)	2.53	0.002
FA 20:2 (n-6)	3.22	0.002
FA 20:3 (n-6)&(n-9)	2.7	0.0059
FA 20:4 (n-6)	1.97	0.0059
FA 20:5 (n-3)	1.69	0.0137
FA 22:0	2.02	0.0098
FA 22:4 (n-6)	3.49	0.002
FA 22:5 (n-6)	2.79	0.002
FA 22:6 (n-3)	2.6	0.002
FA 24:0	2.39	0.0098
FA 24:1 (n-9)	3.43	0.0039
FA 25:0	1.73	0.0488
FA 26:0	2.24	0.0098

PC	c/n	P value
PC 32:1	1.88	0.0039
PC 32:2	3.38	0.0039
PC 34:3	1.48	0.0137
PC 34:5	2.63	0.0039
PC 31:1	4.32	0.0039
PC 33:1	1.99	0.0039
PC 33:2	1.83	0.0039
PC 37:6	1.63	0.0137
PC 30:0	2.34	0.0039
PC 31:0	2.06	0.0098
PC 36:4	0.78	0.0371
PC 36:2e	2.57	0.0195
PC 36:5e	0.68	0.0371
PC 34:4	2.05	0.0059
PC 36:6	2.09	0.0098
PC 33:0	1.51	0.0488
PC 35:1	1.35	0.0137
PC 37:4	0.74	0.0137
PC 39:6	1.49	0.0059
PC 36:1	1.25	0.0195
PC 38:2	1.45	0.0273
PC 40:6	1.28	0.0371
PC 36:1p	1.32	0.0137
PC 34:1e	1.29	0.0273
PC 38:7	1.41	0.0488
PC 36:3e	1.55	0.0371
PC 37:1	1.84	0.0039
PC 37:2	1.71	0.0098
PC 40:7	1.52	0.0195
PC 40:8	1.36	0.0273

LPC	c/n	P value
LPC 14:0 (sn-1)	5.85	0.0039
LPC 14:0 (sn-2)	9.46	0.002
LPC 15:0 (sn-1)	7.97	0.0039
LPC 15:0 (sn-2)	5.64	0.0059
LPC 16:0 (sn-1)	2.99	0.002
LPC 16:0 (sn-2)	2.61	0.0059
LPC 16:0e	3.6	0.0059
LPC 16:0p	4.13	0.0195
LPC 16:1 (sn-1)	5.54	0.002
LPC 16:1 (sn-2)	5.14	0.002
LPC 17:0 (sn-1)	6.1	0.0039
LPC 17:0 (sn-2)	3.48	0.0059
LPC 17:1 (sn-1)	5.93	0.002
LPC 17:1 (sn-2)	6.95	0.002
LPC 18:0 (sn-1)	2.89	0.0098
LPC 18:0 (sn-2)	2.86	0.0059
LPC 18:0p	6.43	0.0469
LPC 18:1 (sn-1)	2.66	0.002
LPC 18:1 (sn-2)	3.58	0.0039
LPC 18:2 (sn-1)	2.04	0.002
LPC 18:2 (sn-2)	3.37	0.0039
LPC 19:0 (sn-2)	3.69	0.0488
LPC 20:1 (sn-1)	3.32	0.0039
LPC 20:1 (sn-2)	3.09	0.0195
LPC 20:2 (sn-1)	4.62	0.002
LPC 20:2 (sn-2)	4.54	0.002
LPC 20:3 (sn-1)	2.49	0.002
LPC 20:3 (sn-2)	4.57	0.0039
LPC 20:4 (sn-1)	1.96	0.0273
LPC 20:5 (sn-1)	1.5	0.0371
LPC 22:0	2.48	0.0156
LPC 22:4 (sn-1)	5.85	0.0039
LPC 22:4 (sn-2)	7.44	0.0078
LPC 22:6 (sn-1)	3.05	0.002
LPC 22:6 (sn-2)	5.48	0.0039

PE	c/n	P value
PE 32:2	3.5	0.002
PE 33:1	2.29	0.002
PE 33:2	2.53	0.0273
PE 32:0	1.5	0.0273
PE 32:1	1.57	0.0195
PE 34:0	1.58	0.0371
PE 34:1	1.22	0.0488
PE 36:4p	0.85	0.0273
PE 38:6p	1.25	0.0488
PE 34:2	1.36	0.0371
PE 36:6	1.68	0.0098
PE 35:2	1.61	0.0488
PE 39:5	0.71	0.0098
PE 39:6	1.97	0.0137
PE 40:6	1.63	0.0137
PE 38:5p	0.82	0.0195
PE 36:2	1.32	0.0371
PE 38:4	1.43	0.0371
PE 38:4e	0.67	0.002
PE 38:4p	0.74	0.002
PE 40:4e	0.65	0.0059

LPE	c/n	P value
LPE 16:0 (sn-1)	2.85	0.0273
LPE 16:0 (sn-2)	2.53	0.0137
LPE 17:0 (sn-1)	4.73	0.0078
LPE 17:0 (sn-2)	3.66	0.0195
LPE 18:0 (sn-1)	3.11	0.0039
LPE 18:0 (sn-2)	2.8	0.002
LPE 18:1 (sn-1)	2.46	0.002
LPE 18:1 (sn-2)	3.52	0.0039
LPE 18:2 (sn-1)	2.15	0.002
LPE 18:2 (sn-2)	4.37	0.002
LPE 20:0 (sn-2)	3.01	0.0137
LPE 20:1 (sn-1)	3.48	0.0273
LPE 20:1 (sn-2)	5.08	0.0195
LPE 20:3 (sn-1)	3.81	0.002
LPE 20:3 (sn-2)	4.91	0.0371
LPE 20:4 (sn-1)	1.64	0.0039
LPE 20:5 (sn-1)	1.9	0.0137
LPE 22:6 (sn-1)	2.32	0.002

AC	c/n	Pvalue
AC 4:0	1.31	0.0371
AC 14:0	4.16	0.0098
AC 16:0	2.4	0.0098
AC 18:0	2.42	0.0273
AC 18:1	1.99	0.0273

The number indicates the relative levels of metabolites adjusted by tissue weight and internal standard and the normalized to the relative levels seen on the normal tissues (c/n: Cancer/Normal). The p-values were evaluated using Mann-Whitney U test. Ether-linked lipid species are labeled with 'e' (plasmanyl) or 'p' (plasmenyl). FA, fatty acid; AC, acylcarnitine; LPC, lysophosphatidylcholine; PC, phosphatidylcholine; LPE, lysophosphatidylethanolamine; PE, phosphatidylethanolamine.

Figure 1. Overview of the results of LC/MS-based lipid analysis.
The data are based on the differences between the CRC and normal tissue samples (CRC/Normal). The vertical axis indicates the total unsaturation number. The horizontal axis shows lipid groups and their variants. The length of each bar indicates the total number of carbon atoms. The color of each bar reflects whether the level of the metabolite had increased (red) or decreased (blue). N.D.: not detected. Cho: cholesterol. Cho includes 4-Cholesten-3-one and 5a-Cholestan-3-one. Primary bile acid includes chenodeoxycholic and cholic acid. Secondary bile acid includes ursodeoxycholic acid and lithocholic acid. Conjugated bile acid includes taurocholic acid, taurochenodeoxycholic acid, glycocholic acid, and glycodeoxycholic acid.
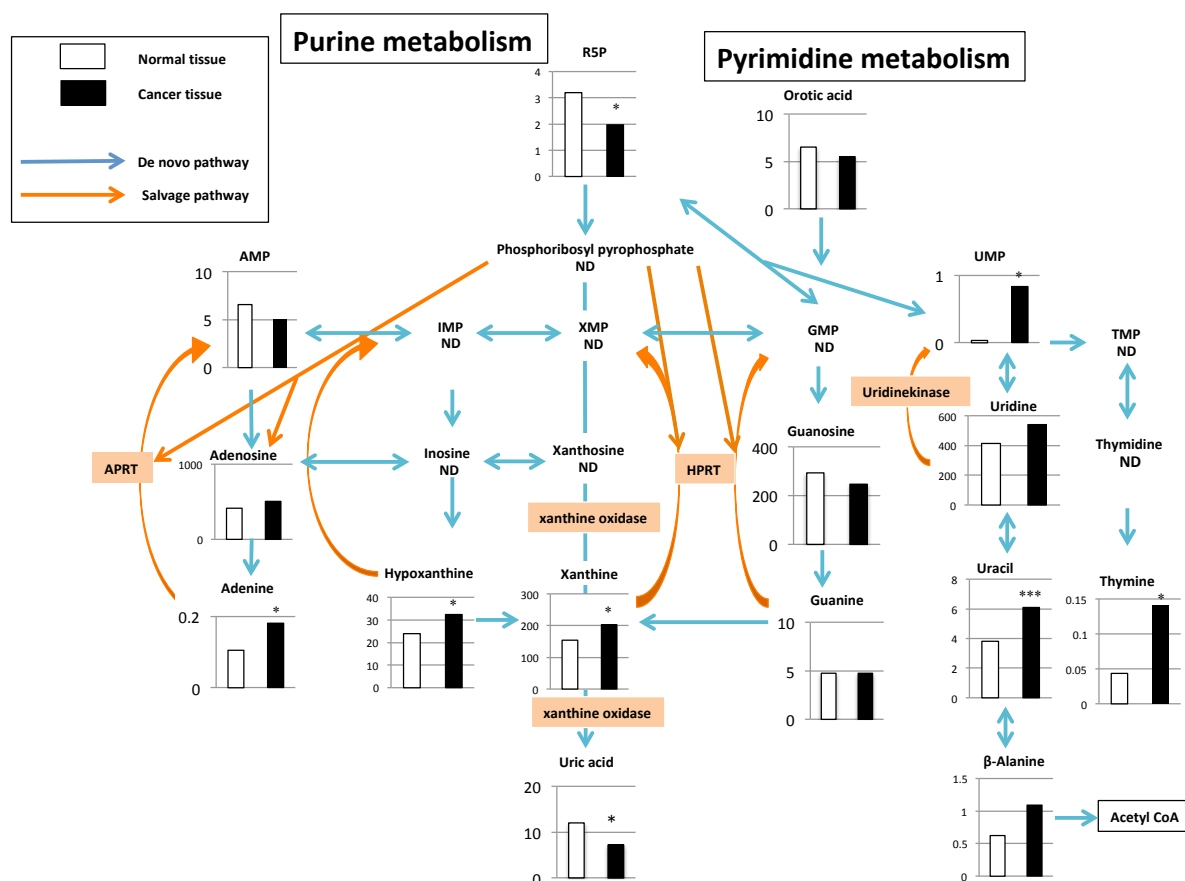
(A)

(B)

Figure 2. Comparison between CRC and normal tissue samples.

(A) Differences in the levels of metabolites related to glycolysis, the TCA cycle, or the surrounding pathways between CRC and normal tissue samples. (B) Differences in the levels of metabolites related to nucleotide *de novo* synthesis or salvage pathways between CRC and normal tissue samples. The values indicate the mean relative levels of metabolites in the CRC or normal tissue samples divided by tissue weight and adjusted for the level of the relevant internal standard. In this figure, the differences in the levels of some metabolites related to glycolysis, the pentose phosphate pathway, the TCA cycle, glutathione biosynthesis, or amino acid pathways between the CRC and normal tissue samples are shown. Adenine, Uracil, Thymine, Hypoxanthine, Hypotaurine, β-Alanine, Taurine, Tryptophan, Glutamine, Glutamic acid, and Putrescine are the results of GC/MS analysis. L-Cystathionine, L-Cysteine, Glycine, L-Ornithine, L-Kynurenine, L-Asparate, L-Asparagine, L-Phenylalanine, L-Serine, L-Threonine, L-Tyrosine, L-Proline, L-Arginine, L-Valine, L-Lysine, L-Leucine, L-Isoleucine, Guanine, Guanosine, Uric acid, Uridine, Adenosine, and Xanthine are the results of LC/MS-based cation analysis. UMP, AMP, Orotic acid, S7P, 6-Phosphogluconic acid, R5P, Ru5P/Xu5P, G1P, G6P, F6P, 2-Phosohogleceric acid, PEP, Pyruvic acid, DHAP, Quinolinic acid, NAD, Malic acid, Oxalic acid, Fumaric acid, and Succinic acid are the results of LC/MS-based anion analysis. The p-values were calculated using the Mann-Whitney U test (*p <0.05; **p <0.01; ***p <0.005). The white and black bars show the results for the normal and CRC tissue samples, respectively. Ketogenic amino acids, glucogenic amino acids, and ketoglucogenic amino acids are indicated in blue, red, and green, respectively. PEP: phosphoenolpyruvic acid, TKT: transketoaldolase, TDLO: transaldolase 1, CDO: cysteine dioxygenase, IDO: indolamine-2,3-dioxygenase, QPRT: quinolinate phosphoribosyltransferase, NAD: nicotinamide adenine dinucleotide, DHAP: dihydroxyacetone phosphate, G1P: glucose 1-phosphate, G3P: glyceraldehyde 3-phosphate, G6P: glucose 6-phosphate, S7P: sedoheptulose 7-phosphate, R5P: ribulose 5-phosphate, Ru5P/Xu5P: xylulose 5-phosphate, PRPP: phosphoribosyl pyrophosphate, F6P: fructose 6-phosphate, HPRT: hypoxanthine-guanine phosphoribosyltransferase, APRT: adenine phosphoribosyltransferase, UMP: uridine monophosphate, TMP: thymine monophosphate, AMP: adenosine monophosphate, ATP: adenosine triphosphate, IMP: inosine monophosphate, XMP: xanthosine monophosphate, R5P: ribulose 5-phosphate.

nucleotide metabolism, the concentrations of adenine, xanthine hypoxanthine, uracil, and thymine were higher, and the level of uric acid was lower in the CRC tissue samples. The levels of adenosine, guanosine, and uridine did not differ significantly between the CRC and normal tissue samples (Figure 2B). To confirm the difference

between non-metastatic and metastatic CRC, we divided 10 samples into 2 groups including non-metastatic CRC (stage I, II) group and metastatic CRC (stage IV) group. In both groups, we could observe the similar tendency about the differences in metabolite levels between the CRC and normal tissue samples, and the tendency was also similar from the results from 10 patients (data not shown). In addition, the ratios between the CRC and normal tissue samples were not significantly different between non-metastatic and metastatic CRC groups (data not shown).

DISCUSSION

Cancer cells rely on altered cellular metabolism to meet their anabolic demands from deregulated cellular growth and aberrant differentiation [4][5]. Cancer cells including CRC have the high proliferative activity, the ability to counter cellular stress in hypoxic conditions [4][9], and the ability to defy the host's immune system, which is a mechanism known as tumor evasion [10][11][12][13]. Our data showed that the levels of metabolites related to antioxidative activity or alternative nicotinamide adenine dinucleotide (NAD) production pathways, for example, taurine and quinolinic acid (QA), were increased in the CRC tissue samples (**Figure 2A**). As for metabolites related to purine metabolism, the level of ribose 5-phosphate was significantly lower in the CRC tissue samples, and the levels of adenine, hypoxanthine, and xanthine were higher in the CRC tissue samples. Concerning the metabolites related to pyrimidine metabolism, significantly higher levels of uridine monophosphate, uracil, and thymine were found in the CRC tissue samples. In contrast, the final product of nucleotide metabolism, uric acid, exhibited lower levels in the CRC tissue samples (**Figure 2B**). Adenosine monophosphate can be converted into adenosine and inosine, which are then broken down into hypoxanthine, xanthine, and uric acid by xanthine oxidoreductase (XOR). XOR catalyzes the last two steps of purine catabolism, which utilizes O_2 and NAD^+ [14]. Michael D. Williams and Xing Zhang showed that the level of hypoxanthine was elevated in normal cells under hypoxic conditions and suggested that elevated levels of hypoxanthine in CRC cells are consistent with increases in oxidative stress [4]. Therefore, the higher level of hypoxanthine in the CRC tissue samples might suggest that CRC is subjected to oxidative stress.

The supply of amino acids to tissues via the bloodstream is pivotal for cancer cell proliferation because cancer cells use some amino acids as energy sources and as a resource for cancer growth [5]. Consistent with our previous findings, in which CRC patients were subjected to serum metabolome analysis [2], the CRC tissue samples displayed the significantly lower level of tryptophan and higher levels of downstream metabolites of tryptophan, such as kynurenine, QA, cystathionine, cysteine, hypotaurine, and taurine, which are antioxidants (**Figure 2A**). Tryptophan, which is an essential amino acid, is critical for cell proliferation. It plays a central role in creating an immunosuppressive environment and is metabolized through the TK pathway [12][13]. Thus, detection of tryptophan depletion and kynurenine accumulation were important findings of the present study. T lymphocytes (T-cells) are extremely sensitive to tryptophan shortages [15]. Tryptophan depletion is related to T-cell anergy and apoptosis, whereas kynurenine suppresses T-cell differentiation and function. Thus, tryptophan depletion and kynurenine accumulation cooperate to mediate immunosuppression in tumors [9]. The accumulation of tryptophan catabolites, such as kynurenine and QA, can result in the generation of niacin and nicotinamide as alternative substrates for NAD synthesis in a step involving quinolinate phosphoribosyltransferase (QPRT) and nicotinamide phosphoribosyltransferase. The TK pathway has been established as a de novo pathway for NAD+ synthesis in the liver and kidneys. As such, cancer cells rapidly consume NAD, which means that they need more energy and require alternative NAD synthesis pathways to the pathway involving nicotinamide [12][16]. In CRC, reactive oxygen species (ROS) produced by immune cells and inflamed epithelia are the primary sources of DNA damage [12]. Once a neoplasm begins to form in the colon, immune cells are invariably recruited to the tumor site. In our study (**Figure 2A**), the levels of kynurenine and QA were increased in the CRC tissue samples, but the levels of nicotinic acid and NAD did not differ significantly between the CRC and normal tissue samples. These results indicate that in the CRC tissue samples, large amounts of tryptophan were metabolized to QA to produce NAD, but NAD was consumed aggressively. QA, which is a precursor to NAD, was identified as an important factor in conferring resistance to oxidative stress on gliomas. It was reported that glioma cells that expressed high levels of QPRT resisted chemotherapy-induced apoptosis by inducing NAD synthesis [9]. CRC cells also express QPRT [17]; therefore, the same process is expected to occur in CRC, and NAD synthesis through QA might increase the resistance of CRC to oxidative stress. Inhibiting QPRT might suppress its protective effect against oxidative stress, which is caused not only by the lack of blood flow in the local CRC environment, but also by chemotherapy and radiotherapy.

Cysteine, which is the rate-limiting amino acid for glutathione synthesis and is the major cellular antioxidant in mammals, is converted into hypotaurine, which is subsequently oxidized to taurine, sulfate, and hydrogen sulfide (H_2S) [18][19][20]. H_2S serves to maintain the cellular bioenergetics of CRC, and promotes angiogenesis

and vasorelaxation, which provides such tumors with blood and nutrients [21]. H_2S might also activate anti-inflammatory and antioxidant pathways and have protective effects against oxidative stress [22]. In the current study (**Figure 2A**), the higher levels of cystathionine, cysteine, hypotaurine, and taurine detected in the CRC tissue samples might indicate that a beneficial microenvironment (for CRC), involving vasodilation and angiogenesis, was induced in the CRC via H_2S and that antioxidant activity was induced via SAA [19][21]. In addition to glutathione and cysteine, taurine plays an important role in antioxidant activity in the body, especially in the intestines, which are constantly exposed to endogenous and exogenous diet-derived oxidants. Taurine is related to bile acid conjugation and also aids lipid absorption. In addition, it helps to maintain cell membrane stability and protects cells [23][24]. Combining these findings with our results, increased levels of taurine might aid lipid absorption and protect CRC cells from oxidative stress. We also observed 2.5 and 1.49 times higher levels of ascorbic acid and pantothenate, respectively, in the CRC tissue samples. Ascorbic acid, which is an antioxidant, protects cells against oxidative stress induced by ROS [25], so increased levels of ascorbic acid might have antioxidant effects in CRC tissue. Pantothenate contributes to the synthesis of coenzyme A, which is involved in FA synthesis. In our LC/MS analysis, most of the FA exhibited higher levels in the CRC tissue samples, so increased levels of pantothenate might stimulate de novo FA synthesis via coenzyme A. Additionally, for example, PC are also the main source of FA. Phospholipase A_2 cleaves FA from the SN_2 position of phospholipids, leading to the increased levels of lyso-phospholipids and the functions as precursors for various types of eicosanoids [26]. In our data, lower levels of PC36:4, PE36:4p, and PC36:5e and in the CRC tissue samples were observed, and these results may exhibit the results of releasing FA 20:4(n-6) from PC36:4 and PE36:4p and the results of releasing FA20:5(n-3) from PC36:5e. Our LC/MS data also indicated that the levels of AA and EPA were increased in the CRC tissue samples (**Table I**). In addition, the EPA/AA ratio was significantly lower in the CRC tissue samples compared with the normal tissues. EPA antagonistically works to AA, so AA may have more effective activities in the CRC tissue compared with the normal tissue. AA is an important polyunsaturated FA for cell signaling, and it is also a precursor of prostaglandin E2 (PGE2). The level of PGE2 has been shown to be increased in human CRC tissue samples [26][27]. Tumor-derived PGE2 induces kynurenine secretion, which in turn promotes cancer cell invasion [28]. The higher levels of AA detected in the CRC tissue samples in the present study might have been related to increased kynurenine secretion and elevated levels of TK pathway metabolites. The higher levels of antioxidant metabolites, such as cystathionine, cysteine, hypotaurine, taurine, and ascorbic acid, in CRC tissues might protect CRC from oxidative stress.

The results of the present GC/MS and LC/MS-based metabolome analyses of CRC tissue samples suggest that the higher level of taurine stabilizes the cell membranes of CRC cells, and that higher levels of antioxidant metabolites, such as cystathionine, cysteine, hypotaurine, and taurine, protect CRC cells from the surrounding environment and aid the proliferation of CRC cells by regulating their redox status. Cancer cells might have the ability to stabilize themselves and survive the oxidative stress associated with marked superoxide production.

REFERENCES

1. **Bray, F., Ferlay, J., Soerjomataram, I., Siegel, R.L., Torre, L.A., and Jemal, A.** 2018. Global cancer statistics 2018. GLOBOCAN estimates of incidence and mortality worldwide for 36 cancers in 185 countries. CA Cancer J Clin **68**:394-424.
2. **Nishiumi, S., Kobayashi, T., Ikeda, A., Yoshie, T., Kibi, M., Izumi, Y., Okuno, T., Hayashi, N., Kawano, S., Takenawa, T., Azuma, T., and Yoshida, M.** 2012. A Novel serum metabolomics-based diagnostic approach for colorectal cancer. PLoS ONE **7**:e40459.
3. **Nishiumi, S., Kobayashi, T., Kawana, S., Unno, Y., Sakai, T., Okamoto, K., Yamada, Y., Sudo, K., Yamaji, T., Saito, Y., Kanemitsu, Y., Okita, N., T., Saito, H, Tsugane, S., Azuma, T., Ojima, N., and Yoshida, M.** 2017. Investigations in the possibility of early detection of colorectal cancer by gas chromatography/triple-quadrupole mass spectrometry. Oncotarget **8**:17115-17126.
4. **Williams, M.D., Zhang, X., Park, J.J., Siems, W.F., Gang, D.R., Resar, L.M., Reeves, R., and Hill, H.H.,Jr.** 2015. Characterizing metabolic changes in human colorectal cancer. Anal Bioanal Chem **407:**4581-4595.
5. **Hirayama, A., Kami, K., Sugimoto, M., Sugawara, M., Toki, N., Onozuka, H., Kinoshita, T., Saito, N., Ochiai, A., Tomita, M., Esumi, H., and Soga, T.** 2009. Quantitative metabolome profiling of colon and stomach cancer microenvironment by capillary electrophoresis time-of-flight mass spectrometry. Cancer Res **69:**4918-4925.

6. **Yoshie, T., Nishiumi, S., Izumi, Y., Sakai, A., Inoue, J., Azuma, T., and Yoshida, M.** 2012 Regulation of the metabolite profile by an APC gene mutation in colorectal cancer. Cancer Sci **103**:1010-1021.

7. **Sakai, A., Suzuki, M., Kobayashi, T., Nishiumi, S., Yamanaka, K., Hirata, Y., Nakagawa, T., Azuma, T., and Yoshida, M.** 2016. Pancreatic cancer screening using a multiplatform human serum metabolomics system. Biomark Med **10**:577-586.

8. **Okuda, S., Yamada, T., Hamajima, M., Itoh, M., Katayama, T., Bork, P., Goto, S., and Kanehisa, M.** 2008. KEGG Atlas mapping for global analysis of metabolic pathways. Nucleic Acids Res **36**:W423-426.

9. **Sahm, F., Oezen, I., Opitz, C.A., Radlwimmer, B., Deimling, A., Adams, S., Bode, H.B., Guillemin, G.J., Wick, W., and Platten, M.** 2013. The endogenous tryptophan metabolite and NAD+ precursor quinolinic acid confers resistance of gliomas to oxidative stress. Cancer Res **73**:3225-3234.

10. **Platten, M., Wick, W., and Eynde, B.J.** 2012. Tryptophan catabolism in cancer: Beyond IDO and tryptophan depletion. Cancer Res **72**: 5435-5440.

11. **Baren, N., Benoît, J., and Eynde, B.J.** 2015. Tryptophan-degrading enzymes in tumoral immune resistance. Front Immunol **vol.6**:1-9.

12. **Santhanam, S., Alvarado, D.M., and Ciorba, M.A.** 2016. Therapeutic targeting of inflammation and tryptophan metabolism in colon and gastrointestinal cancer. Transl Res **167**: 67-79.

13. **Puccetti, P., Fallarino, F., Italiano, A., Soubeyran, I., MacGrogan, G., Debled, M., Velasco, V., Bodet, D., Eimer, S., Veldhoen, M., Prendergast, G.C., Platten, M., Bessede, A., and Guillemin, G.I.** 2015. Accumulation of an endogenous tryptophan-derived metabolite in colorectal and breast cancers. PLoS ONE **10:**1-9.

14. **Ong, E.S., Zou, L., Cheah, P.Y., Eu, K.W., and Ong, C.N.** 2010. Metabolic profiling in colorectal cancer reveals signature metabolic shifts during tumorigenesis. Mol Cell Proeomics: in press.

15. **Frument, G., Rotondo, R., Tonetti, M., Damonte, G., Benatti, U., and Ferrara, G.B.** 2002. Tryptophan-derived catabolites are responsible for inhibition of T and natural killer cell proliferation induced by indoleamine 2,3-dioxygenase. J Exp Med **196:**459-468.

16. **Braidy, N., Guillemin, G.J., and Grant, R.** 2011. Effects of kynurenine pathway inhibition on NAD metabolism and cell viability in human primary astrocytes and neurons. Int J Tryptophan Res **4:**29-37.

17. **Xiao, X., Wans, L., Wei, P., Chi, Y., Li, D., Wang, Q., Ni, S., Tan, C., Sheng, W., Sun, M., Zhou, X., and Du, X.** 2013. Role of MUC20 overexpression as a predictor of recurrence and poor outcome in colorectal cancer. J Transl Med **11:**1-12.

18. **Robey, I.F.** 2012. Examining the relationship between diet-induced acidosis and cancer. Nutr Metab(Lond) **9:**1-11.

19. **Módis K., Coletta, C., Asimakopoulou, A., Szczesny, B., Chao, C., Papapetropoulos, A., Hellmich, M.R., and Szabo, C.** 2014. Effect of S-adenosyl-L-methionine (SAM), an allosteric activator of cystathionine-β-synthase (CBS) on colorectal cancer cell proliferation and bioenergetics in vitro. Nitric Oxide. **41:**146-156.

20. **Szabo, C., Coletta, C., Chao, C., Módis, K., Szczesny, B., Papapetropoulos, A., and Hellmich, M.R.** 2013.Tumor-derived hydrogen sulfide, produced by cystathionine-β-synthase, stimulates bioenergetics, cell proliferation, and angiogenesis in colon cancer. Proc Natl Acad Sci U S A **110:**12474-12479.

21. **Hellmich, M.R., Coletta, C., Chao, C., and Szabo, C.** 2015. The therapeutic potential of cystathionine β-synthetase/hydrogen sulfide inhibition in cancer. Antioxid Redox Signal **22:**424-448.

22. **Brait, M., Ling, S., Nagpal, J.K., Chang, X., Park, H. L., Lee, J., Okamura, J., Yamashita, K., Sidransky, D., and Kim, M.S.** 2012. Cysteine dioxygenase 1 is a tumor suppressor gene silenced by promoter methylation in multiple human cancers. PLoS ONE **7:**e44951.

23. **Bauchart, T.C., Stoll, B., and Burrin, D.G.** 2009. Intestinal metabolism of sulfur amino acids. Nutr Res Rev **22**:175-187.

24. **Tu, S., Zhang, X., Luo, D., Liu,Z., Yang, X., Wan, H., Yu, L., Li, H., and Wan, H.** 2015. Effect of taurine on the proliferation and apoptosis of human hepatocellular carcinoma HepG2 cells. Exp Ther Med **10:**193-200.

25. **de Carvalho Melo-Cavalcante, A.A., da Rocha Sousa, L., Alencar, M.V.O.B., de Oliveira Santos, J.V., da Mata, A.M.O., Paz, M.F.C.J., de Carvalho, R.M., Nunes, N.M.F., Islam, M.T., Mendes, A.N., Gonçalves, J.C.R., da Silva, F.C.C., Ferreira, P.M.P., and de Castro E Sousaa, J.M.** 2019. Retinol palmitate and ascorbic acid: Role in oncological prevention and therapy. Biomed Pharmacother **109:**1394-1405.

26. **Das, S., Martinez, L.R., and Ray, S.** 2014. Phospholipid Remodeling and Eicosanoid Signaling in Colon Cancer Cells. Indian j Biochem Biophy **5**: 512-519.

27. **Neoptolemos, J.P., Husband, D., Imray, C., Rowley, S., and Lawson, N.** 1991. Arachidonic acid and docosahexaenoic acid are increased in human colorectal cancer. Gut **32:**278-281.

28. **Beloribi, S.D., Vasseurand, S., and Guillaumond, F.** 2016. Lipid metabolic reprogramming in cancer cells. Oncogenesis **5:**1-10.